



Influence of Hygrothermal Effect on the Mode II Fracture Toughness of Epoxy Resins for Civil Engineering Applications

Francesco Ascione¹(✉), Luigi Granata¹, Liberata Guadagno², and Carlo Naddeo²

¹ Department of Civil Engineering, University of Salerno, Via Giovanni Paolo II, Fisciano, SA, Italy
fascione@unisa.it

² Department of Industrial Engineering, University of Salerno, Via Giovanni Paolo II, Fisciano, SA, Italy

Abstract. This paper presents the first experimental results relative to the study of the hygrothermal effect on the mode II fracture toughness of two commercial epoxy resins suitable for civil engineering applications. To this scope, adhesive joints (with adherents in Glass Fiber Reinforced Polymer – GFRP) for End Notch Flexure (ENF) test were produced. In particular, three different kinds of sample were considered: aging samples immersed in sea-water and tap-water at a constant temperature of about 30 °C and unaging specimens.

The results here presented and discussed are the first ones (relative to an immersion time of six months) of a huge experimental program still ongoing consisting of 200 samples in total for an immersion time of fifteen months.

The temperature of the water (about 30 °C) was selected to be lower than the resins glass transition temperature evaluated through the variation of the specific heat capacity of the samples measured with Differential Scanning Calorimetry (DSC) analysis following ASTM E1356 Standard. Experimentally, it was observed an increase of the fracture energy in the first months followed by a decrement.

Parallel to the evaluation of the fracture energy in mode II, the water absorption of each kind of resin and GFRP adhesive sample was also investigated according to EN ISO 62:2008. The experimental results show that the equilibrium value of water absorption of both resins is reached in about one month, while that of GFRP samples depends on the type of liquid: three months for tap water and about 5 months for sea water.

Keywords: End Notch Flexure (ENF) test · Water absorption · Epoxy resin · Glass Fiber Reinforced Polymer (GFRP)

1 Introduction

The demand for fibre reinforced polymer (FRP) composites, either for new construction or for rehabilitation of existing structures, has been steadily increasing, especially for applications in aggressive environmental conditions (Keller 2001, Bakis et al. 2002

and Wang et al. 2016). Pultruded Glass Fibre Reinforced Polymer (GFRP) profiles, in particular, are being used in a growing number of applications, including structural parts or components of bridges and buildings (Schaumann et al. 2008, Mara et al. 2014, Keller et al. 2015, Manalo et al. 2017, Daniel 2010).

In outdoor applications, compared to conventional materials, pultruded GFRP profiles offer low self-weight, high specific strength, ease of handling, durability and low maintenance requirements. This makes them particularly well suited for harsh environments, such as waste water facilities, coastal areas and bridges in cold regions (Keller 2001, Bakis et al. 2002); despite their higher initial costs, it has been shown that comparable life cycle costs and less ecological impact can be reached compared to conventional solutions (Daniel 2010).

Although bolted connections are still the most frequent joining technique, bonded connections offer significant advantages, namely the reduction of stress concentrations in the vicinity of bolts and the inexistence of holes (Zhou and Keller 2005, Ascione et al. 2017, Ascione et al. 2018, Razaqpur et al. 2019). For FRP adherends, further advantages stem from the compatibility between the polymer matrix and the adhesive. However, among other concerns (e.g., the behaviour at elevated temperature), a wider use of bonded joints is pending on obtaining a better understanding of their long-term behaviour. This paper presents the first experimental results obtained about the effect of hygrothermal ageing on the fracture energy in mode II of two epoxy resins very often used in construction applications: SikaDur 30 and Araldite. In particular, the results presented are relative to the first six months for SikaDur 30 and four months for Araldite respect to the overall time of fifteen months. The hygrothermal ageing was conducted for two different environments, sea water and tap water, at about 30 °C. The temperature of the water was selected to be lower than the resins glass transition temperature (about 55 °C for SikaDur 30 and 70 °C for Araldite) evaluated through the variation of the specific heat capacity of the samples measured with Differential Scanning Calorimetry (DSC) analysis following ASTM E1356 Standard. Parallel to the evaluation of the fracture energy in mode II, the water absorption was also investigated according to EN ISO 62:2008. The experimental results show that the equilibrium value of water absorption of both resins is reached in about one month, while that of GFRP samples depends on the type of liquid: three months for tap water and about 5 months for sea water.

2 Experimental Details

2.1 Materials

The adhesives investigated in this study were two bi-component paste epoxy adhesives commercially named SikaDur 30 and Araldite produced by Sika and Huntsman, respectively. As recommended by supplier's documentation the following mixing weight ratio were adopted: 1:3 for SikaDur30 and 1:1 for Araldite. Both components were hand-mixed with a spatula until a homogeneous aspect was obtained. The mixing and the curing were performed for both resins at room temperature (RT, about 21 °C) for seven days (SikaDur30) and 1 day (Araldite) as recommended by the supplier.

A key parameter in the testing of adhesive joints is the evaluation of the Glass Transition Temperature (T_g). When adhesively bonded joints are tested below this temperature,

the adhesive behaves like a low-strain rigid material while above this temperature it has a more rubber-like behavior.

The glass transition temperature (T_g) of two epoxy adhesives has been evaluated by thermal analysis performed with a Mettler DSC 822 differential scanning calorimeter in a flowing nitrogen atmosphere. The samples were analyzed by a three-step dynamic heating program in the temperature range 0–350 °C considering a first step from 0 up to 280 °C with a scan rate of 10 °C min⁻¹, a second cooling step from 280 to -50 °C with a scan rate of 50 °C min⁻¹ and a third step from -50 up to 350 °C with a scan rate of 10 °C min⁻¹. The use of such a dynamic heating program allows detecting both the characteristic thermal transitions and the Curing Degree (CD) of the two different epoxy adhesives.

Figure 1 shows the results of the calorimetric experiments related to the thermal transitions manifested by the adhesives. The two thermal traces show a second-order phase transition which identifies the glass transition temperature (T_g) value of the analyzed epoxy adhesives. The T_g values of the two analyzed systems, Araldite and SikaDur 30, are about 70 °C and 45 °C, respectively.

Generally, the range of temperature corresponding to glass transition is strongly dependent on the nature of the components, level of chemical crosslinks, physical chain entanglements in the system, as well as the degree of flexibility of the polymer chains themselves. Additionally, T_g can be significantly reduced by moisture absorption, a factor that should be considered from a practical point of view.

The different T_g values found for the two analyzed formulations are most likely due to different density of the crosslinking network. The DSC thermograms of the two formulations highlight a higher crosslinking density of the Araldite-based resin with respect to the SikaDur 30 system. Therefore a higher value of thermal energy (high T_g) is required for the Araldite system to activate mobility of the chain segments; this makes this system suitable for applications where a higher value of T_g is required.

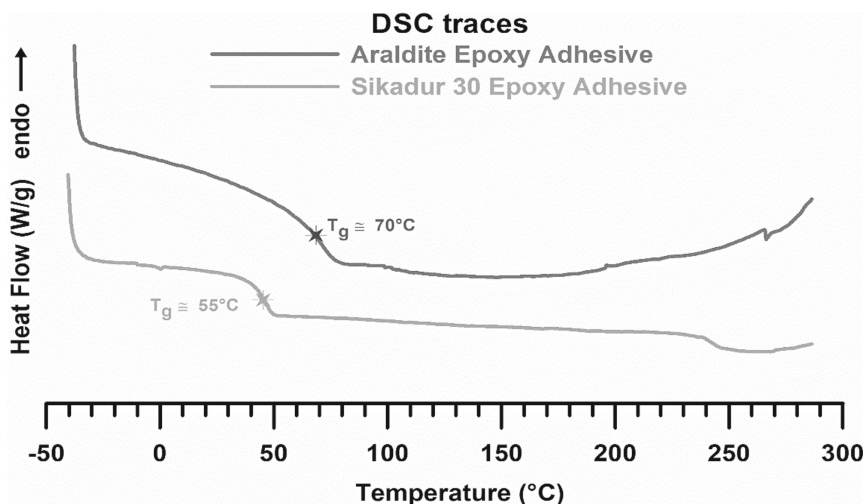


Fig. 1. Glass transition temperature (T_g) of different epoxy adhesives

2.2 Specimen Fabrication

In order to evaluate the fracture energy in Mode II, the End Notch Failure Test (ENF), considered in the literature the most suitable characterization test (de Moura 2009), was adopted.

The ENF test pieces consist of two GFRP plates bonded with the two structural epoxy adhesives above mentioned. GFRP plates were 10 mm thick (t), 25 mm wide (b) and 340 mm long (L_s) as depicted in Fig. 2. The Young Moduli of plates along the fiber direction and that one in transversal direction were 24 GPa and 7 GPa, respectively, while the shear modulus was 3 GPa.

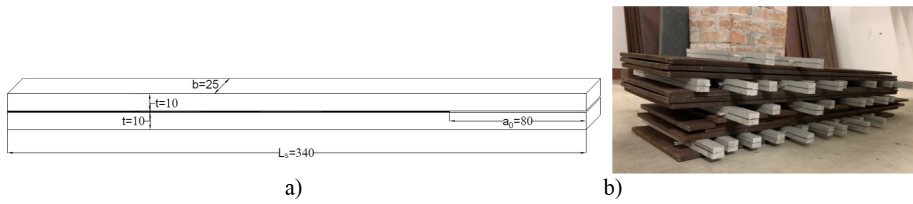


Fig. 2. ENF specimen geometry, a) schematic of the sample, b) photo.

Before bonding, surfaces were grit blasted and degreased with acetone prior to the application of the adhesive. Being the joint symmetric a pure mode II characterization is expected (de Moura and de Morais 2008). The bondline thickness was nominally 1.0 mm. Spacers (calibrated steel bars of 1.0 mm) were inserted between the adherends before the application of the adhesive in order to control the bondline thickness. A pre-crack 80 mm long (a_0), as depicted in Fig. 2, in the adhesive layer was assured in order to have a stable crack growth as reported by Carlsson et al. 1986. In fact, the authors suggested to this scope to adopt an initial crack larger than a critical value equal to 0.35 L (2 L is the span of Fig. 3).

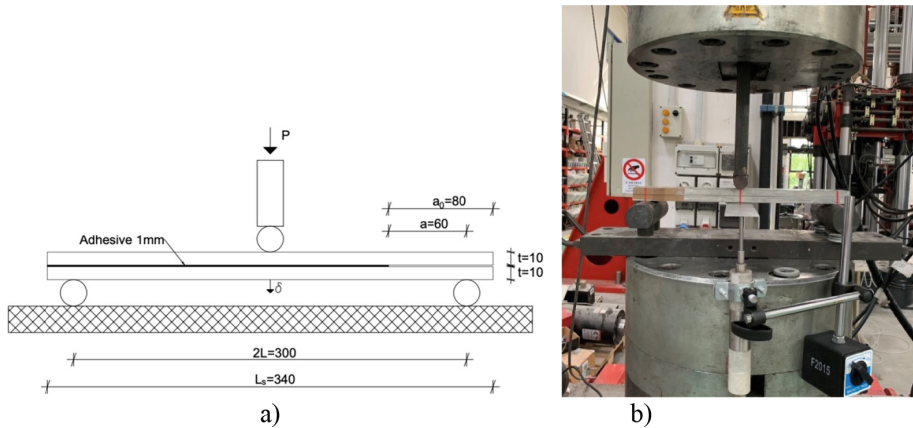


Fig. 3. ENF test geometry, a) schematic representation, b) photo.

2.3 Test Procedure

A schematic representation of the ENF test is shown in Fig. 3. The evaluation of fracture data is based on global force-displacement measurements. The sample was loaded with a force, P , normal to the bondline, applied at the mid-span position, in displacement control at a rate of 0.25 mm/min.

Vertical displacement was measured by a LVDT sensor placed under the specimen at the same cross section where the load was applied (Fig. 3). The distance between the supports (span $2L$) was 300 mm. The joint was loaded continuously until fracture initiated followed by a stable propagation. Three joints (at least) were tested up to failure per each month and resin.

The experimental apparatus shown in Fig. 4 was used for conditioning. It consists of a two separate plastic boxes containing sea water (sw) and tap water (tp), respectively, both at a constant temperature of about 30 °C. The salinity, the temperature and the pH of the sea water were continuously recorded by a redoximeter HI9829 and their distributions over the time are depicted in Fig. 5. For the sake of clarity, oscillations of temperature and salinity are justified by the need for adding cold water in order to maintain the salinity in the range 36–39 PSU (typical values for the Mediterranean sea) due to evaporation phenomenon.

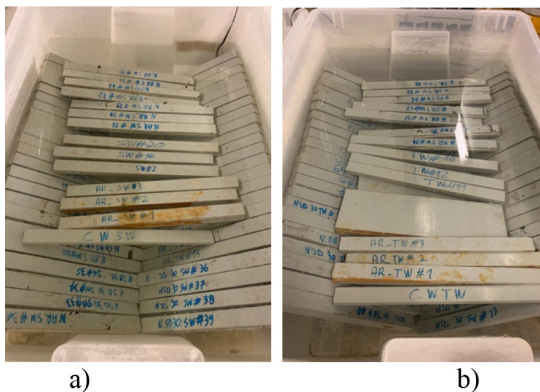


Fig. 4. Immersion apparatus, a) sea water box, b) tap water box.

For what concerns the tap water, the authors monitoring continuously the temperature (average value of 27.95 °C) and the pH (average value of 7.72).

2.4 ENF and Absorption Data Analysis

For the evaluation of fracture energy in mode II (G_{II}) the Compliance-Based Beam Method (CBBM) developed by de Moura et al. 2009 was adopted. This method is based on the crack equivalent concept, depending only on the specimen's compliance during the test. Thus, it does not require crack length monitoring during crack growth which was observed to be very difficult to perform with accuracy in the ENF test. In addition,

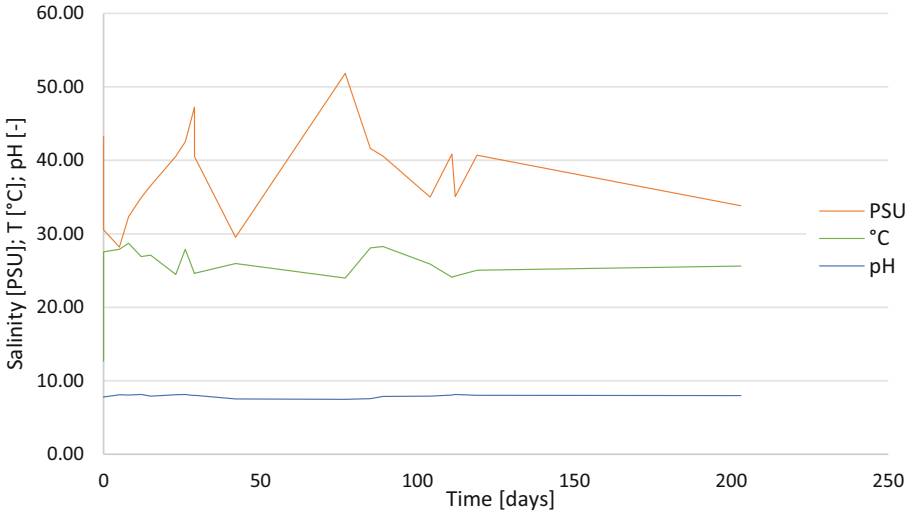


Fig. 5. Graphs for sea water of salinity, temperature and pH vs time.

the equivalent crack length, a_{eq} , accounts for the Fracture Process Zone (FPZ) effects at the crack tip, which is not taken into account when the real crack length is considered. G_{II} can be obtained by the following expression:

$$G_{II} = \frac{9P^2 a_{eq}^2}{16b^2 E_{eq} t^3} \tag{1}$$

where P is the load applied, E_{eq} is an equivalent flexural modulus calculated from the initial compliance and initial crack length, b is the specimen width and t is the thickness of the adherent.

The moisture uptake content (M_t) absorbed by each resin and/or specimen was calculated according to its weight before exposure (w_0) and after exposure (w_t) as follows:

$$M_t = 100 \times \left(\frac{w_t - w_0}{w_0} \right) \tag{2}$$

3 Experimental Results and Discussion

3.1 Water Absorption

Water absorption in the resins is shown in Fig. 6 for both type of conditioning considered. The curves reported are the average one (three samples per each adhesive were monitored). As expected, the rate of water absorption increases with immersion time showing a high incorporation rate at early stages and then continued to incorporate water at a smaller rate. In particular, w_t final intakes were higher than that of sw for both resins.

More in details, SikaDur 30 final intakes were 0.71% and 0.78% for sw and tw, respectively (with a difference equal to 9%). While, for Araldite the final intakes were 3.54% and 4.06% for sw and tp, respectively (with a difference equal to 15%). In general, it is possible to conclude that water intake for Araldite is 5 times bigger than that of SikaDur 30 irrespective of the type of liquid.

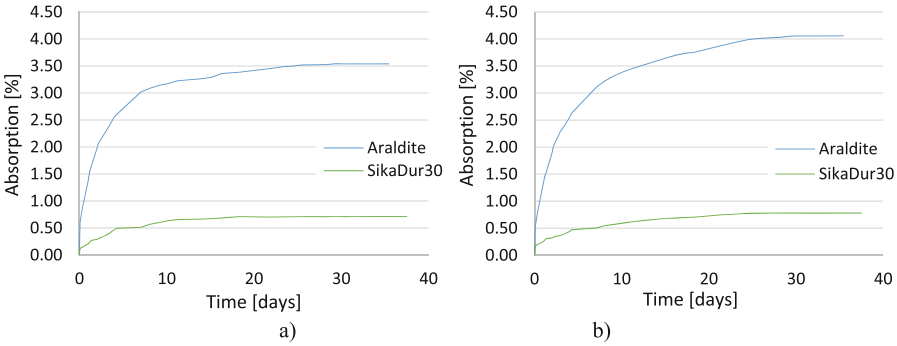


Fig. 6. Water uptake curves for epoxy resins, a) seawater, b) tap water.

As for the resins, in Fig. 7 the water absorption of ENF adhesive joints is reported. Also in this case the curves reported are the average one (three joints per each adhesive were monitored). As mentioned before, immersion time for joints with SikaDur 30 was six months while that one for joints with Araldite was four months. ENF joints present the same final water intake irrespective of adhesive used: about 3.0% for SikaDur 30 and 3.5% for Araldite. A further important result is that seawater reduces drastically the intakes at early stages making longer the period of immersion to reach the final intake respect to the tap water. Considering the results for joints with SikaDur 30 only, the final intake for sw needs for five months instead of three months for tw.

Some authors attributed this phenomenon to the presence of salt in aqueous solutions results in a lower equilibrium content, by virtue of its lower chemical activity. Another

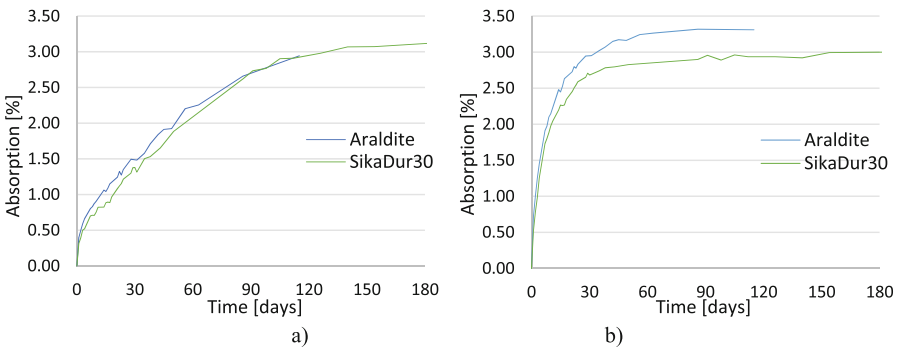


Fig. 7. Water uptake curves for GFRP samples, a) seawater, b) tap water.

possibility is that salts that cover the surfaces of GFRP adherends obstruct the water permeation through the material.

The moisture diffusion here presented (both for resins and joints) could be modelled by the one dimensional Fick model obtaining a perfect agreement between numerical and experimental results. For the sake of brevity, this comparison was not reported in this paper.

3.2 Determination of G_{II} as Function of Immersion Time

Representative experimental $P-\delta$ curves of the ENF specimens for epoxy resins used are reported in Fig. 8. The load increases until the crack initiation process is completed. After that, the crack tip starts propagating. A continuous drop in the force is seen as the crack continuously propagates until the crack reaches the ENF specimen's middle (at the time the crack approaches the loading cylinder, the load starts to increase due to the compression near the crack tip, which obstruct propagation because of friction effects). From Fig. 8 it can be seen that the behavior between SikaDur 30 and Araldite is different. In the first case, the adhesive shows a linear elastic behavior up to failure followed by a vertical drop (brittle behavior) while in the second case the presence of a plastic zone leads to a ductile behavior.

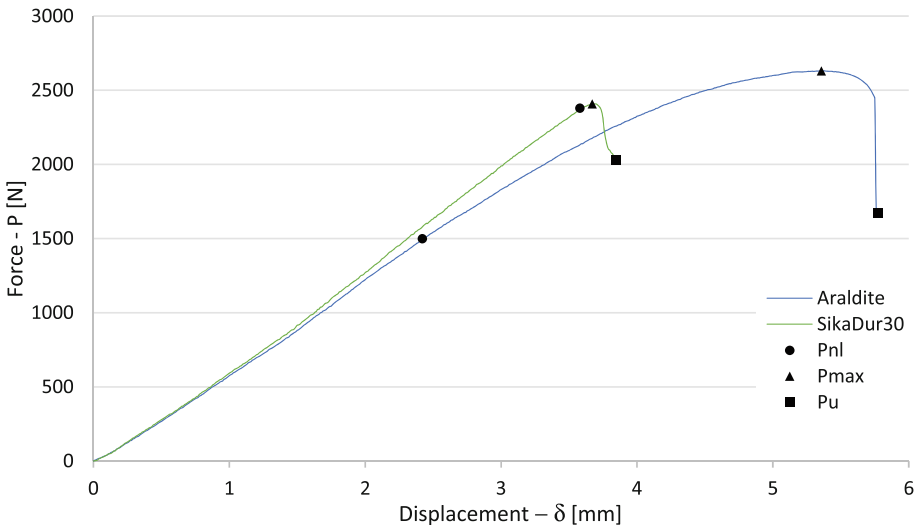


Fig. 8. Representative experimental $P-\delta$ curves of ENF specimens for both epoxy resins (SikaDur 30 and Araldite).

The critical fracture energy in Mode II, G_{II} , was estimated using the CBBM method presented previously. Representative experimental R-curves for ENF specimens are presented in Fig. 9. The ductile behavior of Araldite respect to the brittle behavior of SikaDur 30 is again evident in this Figure considering the increase of the fracture energy when the crack propagates. In particular, the R-curves for Araldite rise rapidly in the initial

stages of crack growth and gradually reach the steady state, (a stable plateau region of approximately constant G_{II}). While, for SikaDur 30, the brittle behavior is represented by a steady state since the initial stages of crack growth (absence of plastic zone).

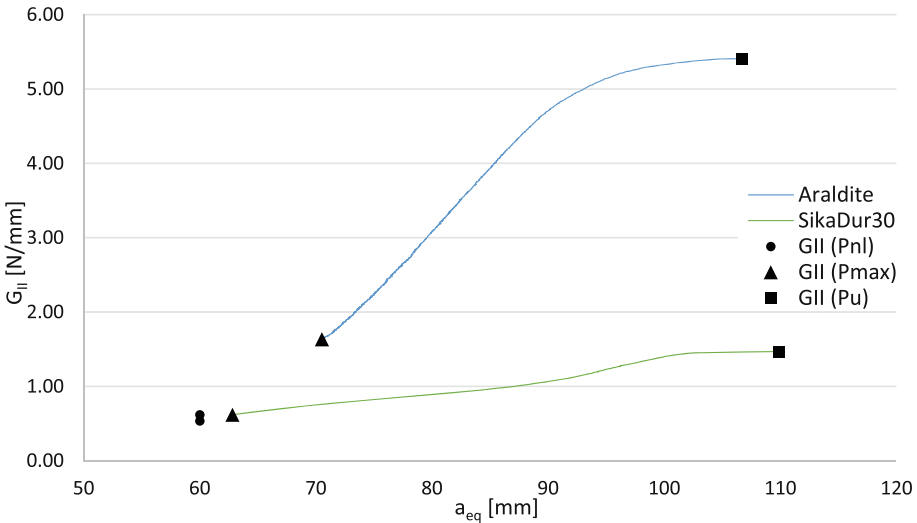


Fig. 9. Representative experimental R-curves of ENF specimens for both epoxy resins (SikaDur 30 and Araldite).

Furthermore, three different values of the fracture energy in mode II were evaluated per each specimen: $G_{II,P_{nl}}$, $G_{II,P_{max}}$ and G_{II,P_u} . In detail, $G_{II,P_{nl}}$ is the fracture energy for the load P corresponding to the loss of linearity (nl stands for non-linear) in the P - δ curve (in this case no FPZ is taken into account and then the equivalent crack length, a_{eq} , coincides with the initial crack, a_0 , equal to 60 mm); $G_{II,P_{max}}$ is the fracture energy for the maximum value of the applied load P (only the initial part of plastic zone is taken into account and a_{eq} is greater than a_0); G_{II,P_u} is the fracture energy for the ultimate value of the load P corresponding to the stop of the crack evolution (crack moves from an unstable state to stable one, the load restarts to increase). In this last case, all FPZ is taken into account and further increments of a_{eq} don't alter the value of the energy fracture (plateau of Fig. 9).

From Fig. 9 it is possible to conclude that the value of fracture energy $G_{II,P_{nl}}$ is the same for both resins.

The effect of immersion time at about 30 °C on the fracture energy toughness is reported in Figs. 10 and 11 for Araldite and SikaDur 30, respectively. Experimentally, it was observed an increase of the fracture energy in the first months followed by a decrement. The results obtained suggest that the temperature of 30 °C play a dual role: it initially activates a post-curing phase with an increase of performance; it subsequently activates irreversible degradation mechanisms (hydrolysis) that produce the drastic reduction of fracture energy.

Per each month, at least three samples were tested in order to evaluate the fracture energy. The values reported in the graphs are the average ones.

From Figs. 10 and 11 it is possible to conclude that the immersion time has an opposite effect on the two resins considered. In detail, the fracture process zone (FPZ) of Araldite vanishes in the first months while, on the contrary, it increases for SikaDur 30. In fact, for Araldite, the initial value of the fracture energy ($G_{II, Pu}$) degrades to the value of $G_{II, Pnl}$ passing from a ductile behaviour to a brittle one; while, for SikaDur 30, the initial value of fracture energy ($G_{II, Pu}$), close to the values of $G_{II, Pnl}$ and $G_{II, Pmax}$ due to the absence of the FPZ, increases faster than the other two, representing an increase of the plastic zone.

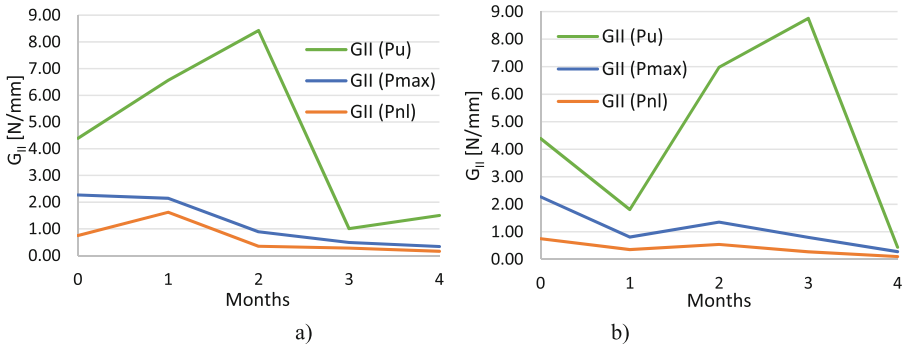


Fig. 10. Araldite fracture energy durability: a) seawater, b) tap water.

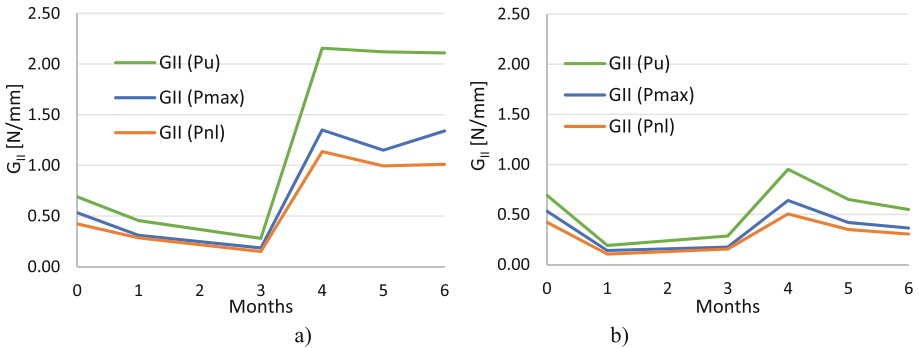


Fig. 11. SikaDur 30 fracture energy durability: a) seawater, b) tap water.

4 Conclusions

The first experimental results relative to the study of the hygrothermal effect on the mode II fracture toughness of two commercial epoxy resins suitable for civil engineering applications are presented and discussed. The evaluation of fracture energy was developed

by the End Notch Flexure (ENF). Two different kinds of conditioning were considered: sea water and tap water at a constant temperature of about 30 °C.

The results reported are the first ones (relative to an immersion time of six months) of a huge experimental program still ongoing consisting of 200 samples in total for an immersion time of fifteen months.

Experimentally, it was observed an increase of the fracture energy in the first months due to the post-curing phase of resin activated by temperature of 30 °C followed by a drastic decrement due to hydrolysis phenomenon.

Furthermore, the water absorption of each kind of resin and GFRP adhesive sample was also investigated. The experimental results show that the equilibrium value of water absorption of both resins is reached in about one month, while that of GFRP samples depends on the type of liquid: three months for tap water and about 5 months for sea water. In general, seawater reduces drastically the intakes at early stages making longer the period of immersion to reach the final intake respect to the tap water. This finding could be due to both the presence of salt in aqueous solutions (resulting in a lower equilibrium content, by virtue of its lower chemical activity) and the possibility that salts cover the surfaces of GFRP adherends obstruct the water permeation through the material.

References

- Keller T (2001) Recent all-composite and hybrid fibre-reinforced polymer bridges and buildings. *Prog. Struct. Eng. Mater.* 3:132–140
- Bakis C, Bank L, Brown V, Cosenza E, Davalos J, Lesko J et al (2002) Fiber-reinforced polymer composites for construction – state-of-the-art review. *J. Compos. Construct.* 6:73–87
- Wang J, GangaRao H, Liang R, Liu W (2016) Durability and prediction models of fiber reinforced polymer composites under various environmental conditions: a critical review. *J. Reinforc. Plast. Compos.* 35:179–211
- Schaumann E, Vallée T, Keller T (2008) Direct load transmission in hybrid FRP and lightweight concrete sandwich bridge deck. *Compos. Part A Appl. Sci. Manuf.* 39:478–487
- Mara V, Haghani R, Harrysin P (2014) Bridge decks of fibre reinforced polymer (FRP): a sustainable solution. *Constr. Build. Mater.* 50:190–199
- Keller T, Theodorou NA, Vassilopoulos AP, De CJ (2015) Effect of natural weathering on durability of pultruded glass fiber–reinforced bridge and building structures. *J. Compos. Construct.* 20:1–9
- Manalo A et al (2017) State-of-the-art review on FRP sandwich systems for lightweight civil infrastructure. *J. Compos. Construct.* 21(1):04016068
- Daniel RA (2010) A composite bridge is favoured by quantifying ecological impact. *Struct. Eng. Int.* 20:385–391
- Zhou A, Keller T (2005) Joining techniques for fiber reinforced polymer composite bridge deck systems. *Compos. Struct.* 69:336–345
- Ascione F, Lamberti M, Razaqpur AG, Spadea S (2017) Strength and stiffness of adhesively bonded GFRP beam-column moment resisting connections. *Compos. Struct.* 160:1248–1257
- Ascione F, Lamberti M, Razaqpur AG, Spadea S, Malagic M (2018) Pseudo-ductile failure of adhesively joined GFRP beam-column connections: an experimental and numerical investigation. *Compos. Struct.* 200:864–873
- Razaqpur AG et al (2019) GFRP hollow column to built-up beam adhesive connection: Mechanical behaviour under quasi-static, cyclic and fatigue loading. *Compos. Struct.* 224:111069

- de Moura MFSF, Campilho RDSG, Gonçalves JPM (2009) Pure mode II fracture characterization of composite bonded joints. *Int. J. Solids Struct.* 46:1589–1595
- de Moura MFSF, de Morais AB (2008) Equivalent crack based analyses of ENF and ELS tests. *Eng. Fract. Mech.* 75:2584–2596
- Carlsson LA, Gillespie JW, Pipes RB (1986) On the analysis and design of end notched flexure (ENF) for mode II testing. *J. Compos. Mater.* 20:594–604